BIOCHEMISTRY
including biophysical chemistry & molecular biology

Article

pubs.acs.org/biochemistry

[2Fe-2S] Proteins in Chlorosomes: Redox Properties of CsmI, CsmJ, and CsmX of the Chlorosome Envelope of *Chlorobaculum tepidum*

T. Wade Johnson,[†,∥] Hui Li,[†,⊥] Niels-Ulrik Frigaard,[†,@] John H. Golbeck,[†,‡] and Donald A. Bryant*[,†,§]

[†]Department of Biochemistry and Molecular Biology, The Pennsylvania State University, University Park, Pennsylvania 16802, United States

[‡]Department of Chemistry, The Pennsylvania State University, University Park, Pennsylvania 16802, United States

[§]Department of Chemistry and Biochemistry, Montana State University, Bozeman, Montana 59717, United States

ABSTRACT: The chlorosome envelope of *Chlorobaculum tepidum* contains 10 polypeptides, three of which, CsmI, CsmJ, and CsmX, have an adrenodoxin-like domain harboring a single [2Fe-2S] cluster. Mutants that produced chlorosomes containing two, one, or none of these Fe−S proteins were constructed [Li, H., et al. (2013) *Biochemistry 52*, preceding paper in this issue (DOI: 10.1021/bi301454g)]. The electron paramagnetic resonance (EPR) spectra, *g* values, and line widths of the Fe−S clusters in individual CsmI, CsmJ, and CsmX proteins were obtained from studies with isolated chlorosomes. The Fe−S clusters in these proteins were characterized by EPR and could be differentiated on the basis of their *g* values and line widths. The EPR spectrum of wild-type chlorosomes could be simulated by a 1:1 admixture of the CsmI and CsmJ spectra. No contribution of CsmX to the EPR spectrum of chlorosomes was observed because of its low abundance. In chlorosomes that contained only CsmI or CsmJ, the midpoint potential of the [2Fe-2S] clusters was −205 or 8 mV, respectively; the midpoint potential of the [2Fe-2S] cluster in CsmX was estimated to be more oxidizing than −180 mV. In wild-type chlorosomes, the midpoint potentials of the [2Fe-2S] clusters were −348 mV for CsmI and 92 mV for CsmJ. The lower potential for CsmI in the presence of CsmJ, and the higher potential for CsmJ in the presence of CsmI, were attributed to interactions that occur when these proteins form complexes in the chlorosome envelope. The redox properties of CsmI and CsmJ are consistent with their proposed participation in the transfer of electrons to and from quenchers of energy transfer in chlorosomes.

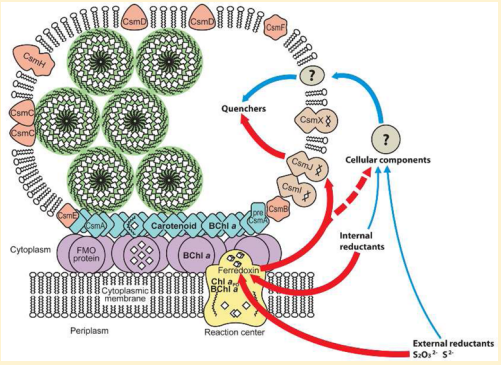

Chlorosomes are highly efficient light-harvesting structures that are found in members of three bacterial phyla that contain green bacterial members: Chlorobi (green sulfur bacteria, GSB), Chloroflexi (filamentous anoxygenic phototrophs, FAPs), and Acidobacteria ("*Candidatus* Chloroacidobacterium thermophilum").[1−5] In the model GSB, *Chlorobaculum tepidum*, chlorosomes contain several coaxial nanotubes assembled from up to 250000 aggregated bacteriochlorophyll (BChl) *c* molecules.[6−9] Chlorosomes additionally contain carotenoids, quinones, wax esters, glycolipids, and a small amount of BChl *a*.[2] An asymmetric, protein-stabilized, glycolipid envelope surrounds the chlorosome, which is attached to the Fenna−Matthews−Olson protein (FMO) by a paracrystalline array of CsmA complexed with BChl *a* and carotenoids.[2,10−12]

Several studies of the structure and organization of the envelope-bound proteins of chlorosomes from *Cba. tepidum* have been performed.[10−14] Highly purified chlorosomes from *Cba. tepidum* contain 10 principal polypeptides (CsmA, CsmB, CsmC, CsmD, CsmE, CsmF, CsmH, CsmI, CsmJ and CsmX).[13−18] These proteins belong to four structural motif families: CsmA/E, CsmC/D, CsmB/F, and CsmI/CsmJ/CsmX. CsmA is the only protein that is essential for the structure and integrity of the chlorosome as well as cellular viability.[13,19,20] Proteins of the CsmC/D and CsmB/F motif families are important in determining the size and shape of chlorosomes, and they may influence the organization of the BChl *c* molecules in the interior.[20] CsmH has been suggested to arise from a combination of an N-terminal CsmB/F domain and a C-terminal CsmC/D domain[14] and exists as dimers in the chlorosome envelope.[10] The CsmI, CsmJ, and CsmX proteins of chlorosomes have an N-terminal domain that resembles adrenodoxin-type, [2Fe-2S] ferredoxins, and they additionally have a CsmA/E domain at their C-termini.[14,18]

The *csmI* and *csmJ* genes of *Cba. tepidum* have been heterologously expressed in *Escherichia coli*, and the resulting proteins have been partly characterized biochemically.[18] CsmI and CsmJ formed inclusion bodies when the genes encoding these proteins were overexpressed in *E. coli*. Nevertheless, preliminary EPR characterization and *g* value simulation of the [2Fe-2S] clusters associated with CsmJ in inclusion bodies and wild-type (WT) chlorosomes were performed (CsmX had not yet been identified and was not examined in these initial experiments). The midpoint potential of the Fe−S clusters associated with CsmJ inclusion bodies was found to be −194 mV.

Received: October 25, 2012
Revised: January 28, 2013
Published: January 31, 2013

A redox titration of the mixture of Fe−S clusters in isolated, WT chlorosomes yielded two midpoint potential values: E_{m1} = −201 mV, and E_{m2} = 92 mV. On the basis of these observations, Vassilieva et al.[18] assigned the lower midpoint potential (E_{m1}) to CsmJ and the higher midpoint potential (E_{m2}) to CsmI. The extremely limited solubility and low cluster occupancy of recombinant CsmI did not allow the midpoint potential of the Fe−S cluster to be determined.

An intriguing property of chlorosomes is that they contain large amounts of quinones, approximately one per 10 BChl *c* molecules, which are chlorobiumquinone (1′-oxo-menaquinone-7), 1′-OH-menaquinone-7, and menaquinone-7 in *Cba. tepidum*.[21,22] It is thought that the oxidized and/or semiquinone forms of these quinones create quenching centers that block the transfer of energy from the BChls in chlorosomes to FMO and reaction centers.[21−26] When oxidized chlorosomes are reduced, energy transfer, as measured by an increase in the amplitude of fluorescence emission, is restored.

This study focused on the EPR characterization of the CsmI, CsmJ, and CsmX proteins in their native environment in the envelopes of isolated chlorosomes. As described in the preceding paper (DOI: 10.1021/bi301454g), mutants were constructed in which one, two, or all three of the genes encoding the Fe−S cluster-containing proteins were insertionally inactivated. Analyses of isolated chlorosomes and intact cells of these mutants strongly suggested that these Fe−S proteins participate in the oxidation and reduction of the redox-activated quencher of energy transfer in chlorosomes. Here, the EPR spectra, *g* values, and line widths of the Fe−S clusters of chlorosomes are reported. The EPR spectrum of WT chlorosomes could be simulated by admixing the EPR spectra in a 1:1 ratio for CsmI and CsmJ and by ignoring any contribution from the minor Fe−S protein, CsmX. Midpoint potentials were determined for the Fe−S clusters in WT chlorosomes, in chlorosomes containing CsmI and CsmJ individually, and in chlorosomes containing two of the three Fe−S proteins. The midpoint potentials observed in WT chlorosomes differed from those of the individual proteins. Furthermore, the midpoint potentials of the Fe−S clusters found in WT chlorosomes differed from those previously reported by Vassilieva et al.[18] The redox potential of the Fe−S clusters in CsmI and CsmJ depended upon the presence of both partner proteins. A probable explanation for the observed variation in redox potentials of these Fe−S clusters will be discussed.

MATERIALS AND METHODS

Strains and Growth Conditions. The WT2321 strain of *Cba. tepidum* (formerly *Chlorobium tepidum*), which is a plating strain derived from *Cba. tepidum* strain ATCC 49652, was used in these studies.[27,28] The media for the growth of *Cba. tepidum* on plates or in liquid cultures were the same as those described previously.[29] The construction of *csmI*, *csmJ*, and *csmX* single mutants was described previously.[19] The construction and verification of the *csmI csmJ*, *csmI csmX*, *csmJ csmX*, and *csmI csmJ csmX* mutants are described in the preceding paper (DOI: 10.1021/bi301454g).

Chlorosome Preparation and Chlorophyll Concentration. Chlorosomes were isolated on 7 to 47% (w/v) continuous sucrose gradients essentially as described previously,[30] except that 1.0 mM phenylmethanesulfonyl fluoride and 2 mM dithiothreitol were present throughout the entire procedure.[10,14] Chlorosomes in pooled fractions from the sucrose gradients were pelleted twice after dilution or resuspension in 50 mM Tris-HCl (pH 8.2) by ultracentrifugation (240000*g* for 1.5 h), which removed sucrose and NaSCN. The BChl *c* concentration was determined by measuring the absorbance of methanol extracts of the chlorosomes using the specific absorption coefficient of 86 L g^{-1} cm^{-1}.[31]

EPR Spectroscopy and Redox Titrations. EPR studies were performed at X-band with a Bruker ECS-106 spectrometer equipped with an ER/4102ST resonator. Cryogenic conditions were maintained with an Oxford Instruments ESR900 liquid helium cryostat, and the temperature was controlled with an ITC4 temperature control unit. The microwave frequency was measured with a Hewlett-Packard 5352B frequency counter.

X-Band EPR spectra were recorded with chlorosomes that had been prepared from anoxic stock samples, which had been stored in 50 mM Tris-HCl (pH 8.2) at −80 °C. Reduced samples were prepared in an anoxic chamber (Coy Laboratory Products, Grass Lake, MI) by the addition of 10 μL of a freshly prepared solution of 0.5 M sodium hydrosulfite in 50 mM Tris-HCl (pH 8.2) to a 0.2 mL sample of chlorosomes stored on ice. The BChl *c* concentrations of typical chlorosome samples was approximately 10 mg/mL, except for measurements with CsmX, when higher concentrations (30−40 mg/mL) were required. Each EPR spectrum shown is the average of five scans recorded at 30 K, with a microwave power of 1.26 mW and a modulation amplitude of 1 mT.

For the redox titration experiments with EPR detection, all solutions were prepared anoxically and were mixed in an anoxic chamber. Chlorosomes were diluted in 50 mM Tris-HCl buffer (pH 8.2) to a BChl *c* concentration of 10 ± 0.5 mg/mL. For chlorosomes isolated from the *csmI csmJ* mutant (i.e., chlorosomes containing CsmX), the analyzed sample had a BChl *c* concentration of 35 ± 0.5 mg/mL. The solution potential was set to a specific value by the addition of 2 μL aliquots of 500, 50, and 5 mM sodium hydrosulfite solutions or 200 and 20 mM potassium ferricyanide solutions. A cocktail of redox mediators stabilized the redox potential. The concentrations of the redox mediators used in these experiments were 50−100 μM. The following mediators were dissolved in water: indigo carmine (−125 mV), benzyl viologen (−358 mV), methyl viologen (−440 mV), 1,8-dichloroanthraquinone (−473 mV), 4,4′-dimethyl-1,1′-trimethylene-2,2′-dipyridinium dibromide (−670 mV), and 1,1′-trimethylene-2,2′-dipyridinium dibromide (−521 mV). The following mediators were dissolved in DMSO, with a final DMSO concentration in the titration sample of <1% (v/v): 2,5-dihydroxybenzoquinone (−80 mV), 2-methyl-1,4-naphthoquinone (−10 mV), 2-sulfate-anthraquinone (−218 mV), 1-nitro-anthroquinone (−363 mV), and 2,3-dichloro-1,4-naphthoquinone (−300 mV). The ambient potential of the solution was measured using a gold and $Ag/AgCl_2$ reference electrode (MF-2052 BAS, West Lafayette, IN) and a high-impedance voltmeter. The reaction vessel was a custom-made, 5 mL Pyrex beaker with a side port for the gold electrode and microflea stir bar for mixing the solution. The vessel was positioned on a magnetic stir plate, and approximately 160 μL of sample, buffer, and redox mediators were mixed. To reduce the sample fully, 1 μL of freshly prepared 500 mM sodium hydrosulfite was added. Aliquots (2 μL) of potassium ferricyanide and sodium hydrosulfite were added to set the potential to a specific value. Once the desired potential had been achieved and had stabilized, the sample was quickly placed into an EPR tube and frozen in liquid nitrogen. Frozen samples could be stored indefinitely at 77 K; however, EPR measurements were usually performed within a few days. Each experiment was repeated two to five times. The midpoint redox potentials were calculated by fitting the

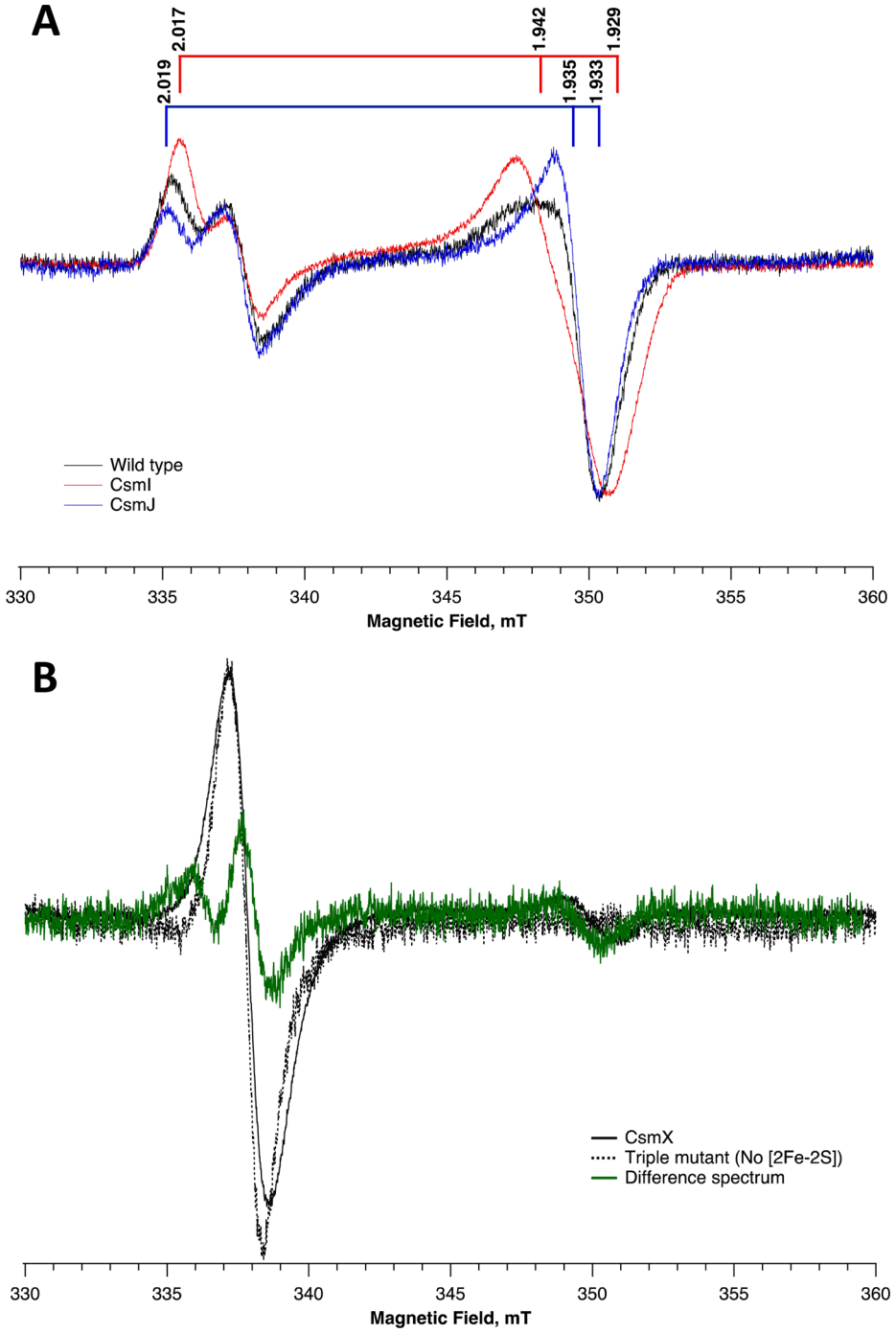

Figure 1. (A) EPR spectra of chemically reduced chlorosomes of *Cba. tepidum* WT, *csmJ csmX*, and *csmI csmX*. The chlorosomes were suspended in 50 mM Tris-HCl (pH 8.2) and reduced by the addition of sodium hydrosulfite to a final concentration of 10 mM. The chlorosome concentrations of the WT, the *csmI csmX* double mutant, and the *csmI csmJ csmX* triple mutant were 10 mg of BChl *c*/mL; for the *csmJ csmX* mutant 15 mg of BChl *c*/mL; and for the *csmI csmJ* mutant 35 mg of BChl *c*/mL. EPR conditions: temperature, 30 K; microwave power, 1.26 mW; modulation amplitude, 1 mT; magnetic field, 3300−3600 G. (B) Difference spectra of the Fe−S cluster in CsmX calculated by subtracting the EPR spectrum of chlorosomes of the *csmI csmJ csmX* triple mutant from that of chlorosomes of the *csmI csmJ* mutant (containing CsmX). The chlorosomes were suspended in 50 mM Tris-HCl (pH 8.2) and reduced by the addition of sodium hydrosulfite to a final concentration of 10 mM. The chlorosome concentration of the *csmI csmJ csmX* triple mutant was equivalent to 10 mg of BChl *c*/mL and for the *csmI csmJ* mutant 35 mg of BChl *c*/mL. EPR conditions: temperature, 30 K; microwave power, 1.26 mW; modulation amplitude, 1 mT; magnetic field, 3300−3600 G. The spectra were normalized to the organic radical with a *g* value 2.0036.

amplitude of the $g = 1.93$ EPR resonance versus the potential of the solution to the sigmoidal curve, which is an equivalent to the Nernst equation for a one-electron transfer per oxidation−reduction process using a nonlinear Marquardt regression algorithm in IgorPro version 4.0 (Wavemetrics, Inc.). All potentials reported here are reported relative to the standard hydrogen electrode (SHE; $Ag/AgCl_2$ = −197 mV). The EPR measurements for the titration experiments were single scans performed at 30 K with a microwave power of 1.26 mW and a modulation amplitude of 1 mT.

dx.doi.org/10.1021/bi301455k | *Biochemistry* 2013, 52, 1331−1343

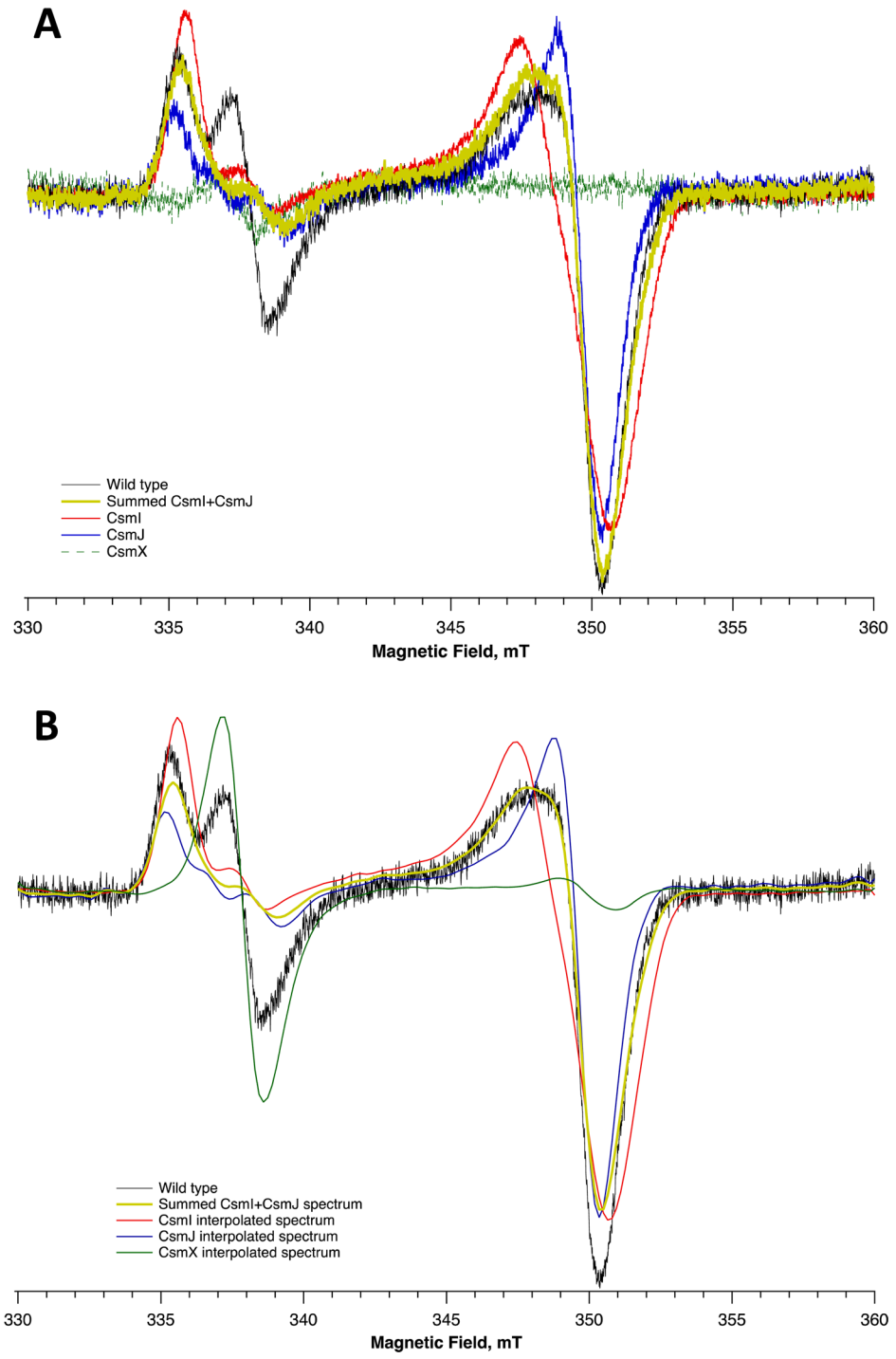

Figure 2. Simulation of the EPR spectrum for *Cba. tepidum* WT chlorosomes produced by directly summing the experimental spectra (A) or by summing smoothed spectra (B) for chlorosomes mutant strains. (A) EPR spectra for chlorosomes from WT *Cba. tepidum* as well as double mutants producing chlorosomes containing only CsmI, CsmJ, or CsmX. The EPR spectrum of WT chlorosomes was accurately simulated by summing the spectra for chlorosomes containing only CsmI and CsmJ. (B) The spectra in panel A were smoothed using a cubic spline interpolation method in Igor Pro version 4.0. The smoothed spectra for chlorosomes containing only CsmI and CsmJ were summed and accurately simulated the spectrum of WT chlorosomes. The g = 2.0036 feature is unrelated to the Fe−S clusters and was not simulated. The chlorosome concentrations for the WT, *csmI csmX* double mutant, and *csmI csmJ csmX* triple mutant were 10 mg of BChl *c*/mL; for the *csmJ csmX* double mutant 15 mg of BChl *c*/mL; and for the *csmI csmJ* double mutant 10 mg of BChl *c*/mL.

RESULTS

EPR Properties of Proteins Containing Fe−S Clusters in Chlorosomes. As previously reported,[18] isolated chlorosomes from WT *Cba. tepidum* have an EPR spectrum that was tentatively assigned to the [2Fe-2S] clusters contained in three of the 10 proteins found in the chlorosome envelope. To resolve the individual spectral components of the Fe−S clusters that form the composite spectrum observed for WT chlorosomes, three double mutants were constructed: *csmJ csmX*, *csmI csmX*, and *csmI csmJ*. Each double mutant produced chlorosomes that

dx.doi.org/10.1021/bi301455k | *Biochemistry* 2013, 52, 1331−1343

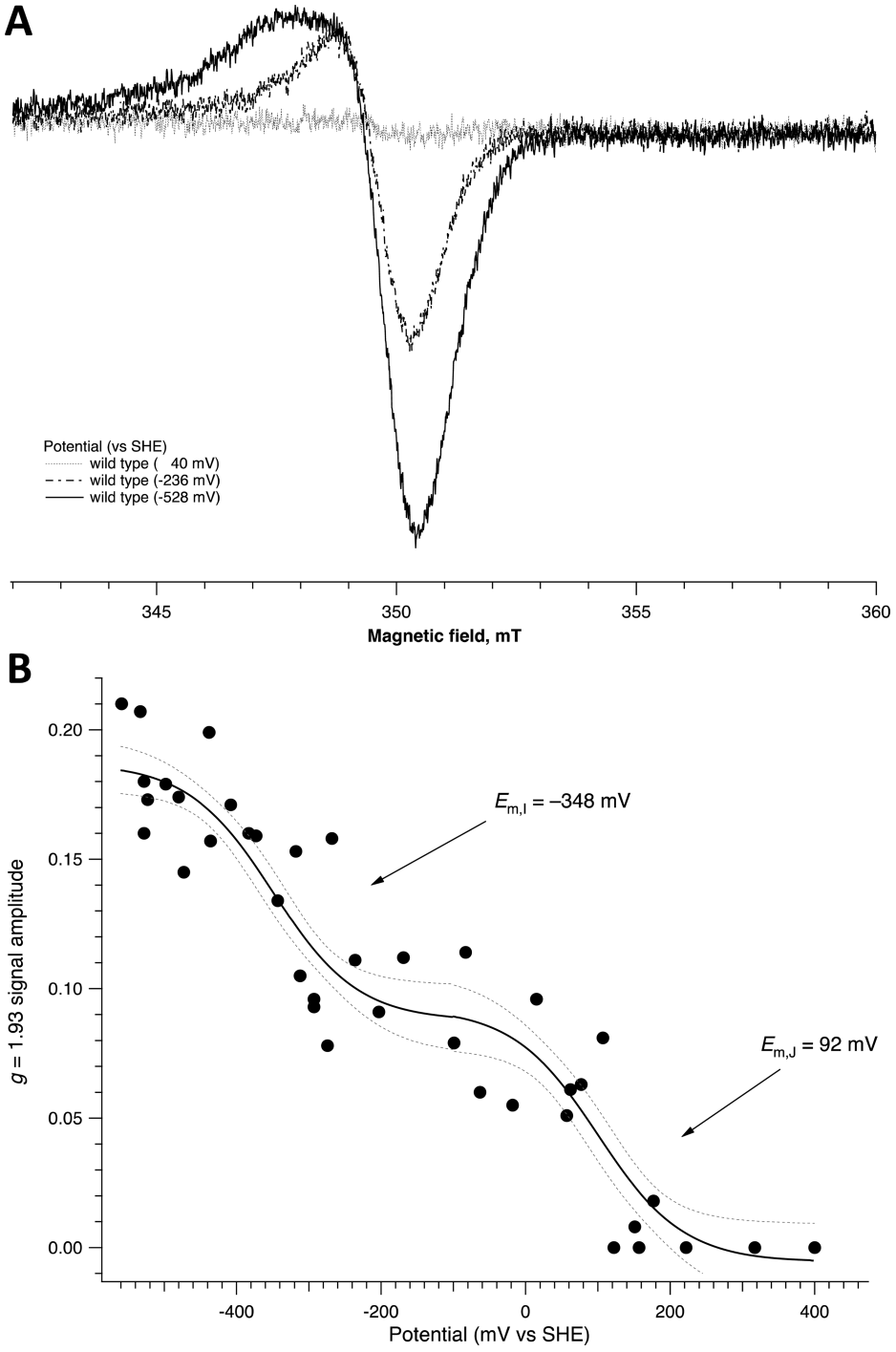

Figure 3. Representative EPR spectra of the WT chlorosomes at different solution potentials (A) and redox titration of isolated chlorosomes from WT *Cba. tepidum* (B). For panel A, the potentials were adjusted stepwise by the addition of 50 mM sodium hydrosulfite (see Materials and Methods). For panel B, the amplitude of the g = 1.93 EPR signal has been plotted against the potential of the solution as measured against the standard hydrogen electrode. Filled circles depict data from one experimental run at a given potential. The calculated curve fits are indicated by a solid line for the reduction potential and one-standard deviation error bars by flanking dashed lines. The curve is fit to a total of 38 points from five individual runs.

contained a single Fe−S protein [CsmI, CsmJ, and CsmX, respectively; see the preceding paper (DOI: 10.1021/bi301454g)]. A *csmI csmJ csmX* triple mutant that contains no Fe−S proteins was also constructed. This strain served as a background control that could be used to identify other EPR signals in chlorosomes that might have interfered with the characterization of the Fe−S proteins.

Figure 1A shows the EPR spectra of isolated chlorosomes from WT *Cba. tepidum*, the *csmJ csmX* mutant (containing only CsmI), and the *csmI csmX* mutant (containing only CsmJ). When chemically reduced with dithionite, the CsmI and CsmJ proteins in chlorosomes exhibited EPR spectra that differed from one another as well as from the spectrum of WT chlorosomes. As determined by numerical simulation, CsmI has principal g values of 2.017, 1.942, and 1.929 (g_{av} = 1.963) and line widths of 0.9, 1.9, and 1.6 mT. Similarly, CsmJ has principal g values of 2.019, 1.935, and 1.933 (g_{av} = 1.962) and line widths of 1.0, 1.5, and 1.3 mT. Figure 1B shows the EPR spectra of isolated chlorosomes from

dx.doi.org/10.1021/bi301455k | *Biochemistry* 2013, 52, 1331−1343

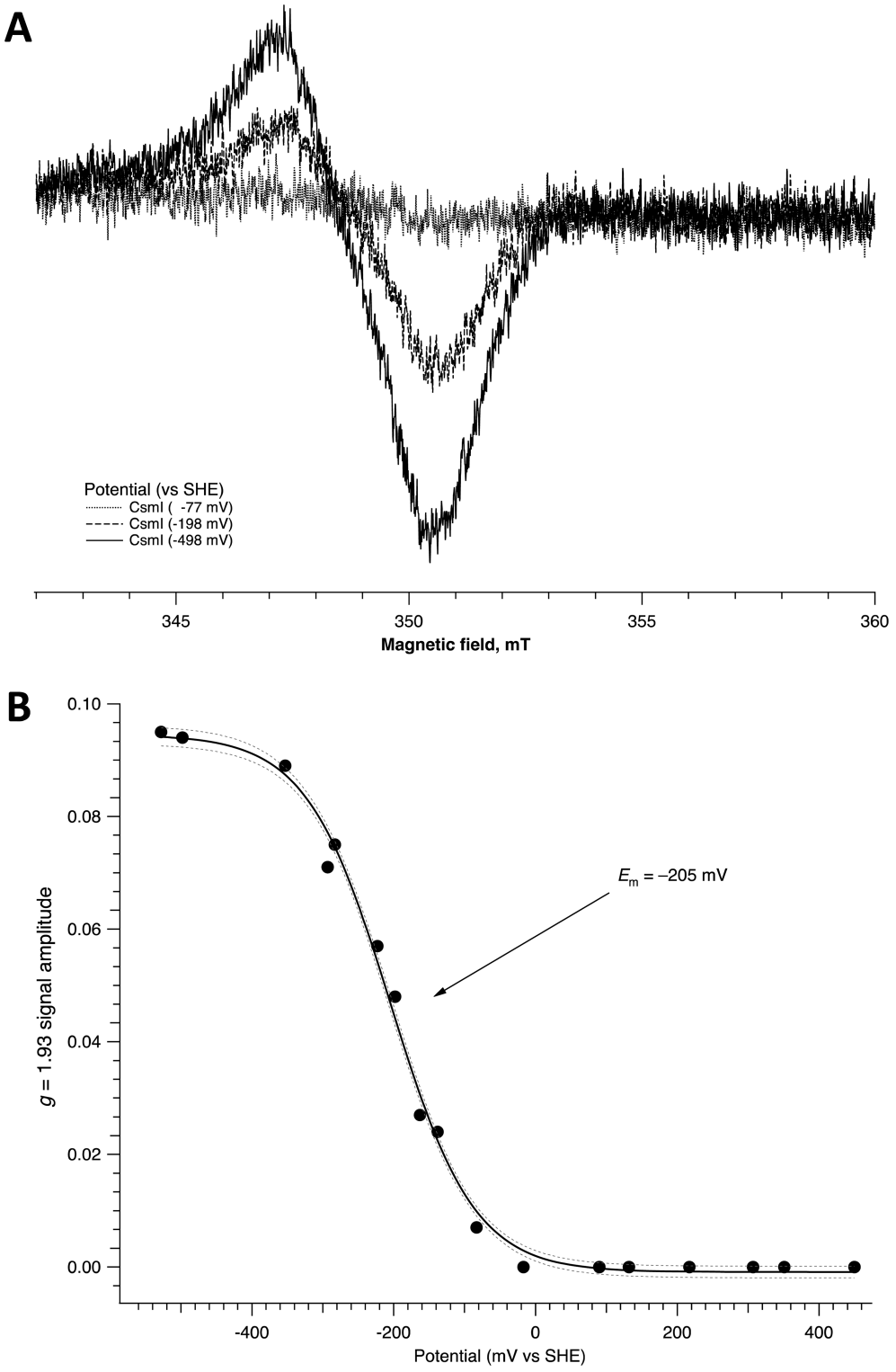

Figure 4. Representative EPR spectra of CsmI-containing chlorosomes at different solution potentials (A) and redox titration of chlorosomes isolated from the *csmJ csmX* mutant (containing CsmI) (B). For panel B, the potentials were adjusted stepwise by the addition of 50 mM sodium hydrosulfite. In panel A, the amplitude of the $g = 1.93$ EPR signal was plotted against the potential of the solution as measured against the standard hydrogen electrode. Filled circles depict data from one experimental run at a given potential. The calculated curve fits are indicated by a solid line for the reduction potential and one-standard deviation error bars by flanking dashed lines. The curve is fit to a total of 17 points from two individual runs.

the *csmI csmJ* mutant (containing only CsmX) and the *csmI csmJ csmX* mutant (containing no Fe−S proteins). At the very high chlorosome concentrations employed (equivalent to >30 mg of BChl *c*/mL), the EPR spectrum is dominated by a radical centered at 337.5 mT, which is not associated with an Fe−S protein. Because of the very low concentration of CsmX (~5% of the level of CsmI and CsmJ combined) in chlorosomes (DOI: 10.1021/bi301454g), which resulted in a low signal-to-noise ratio, the EPR spectrum of CsmX could not be completely resolved. The difference spectrum between the normalized

dx.doi.org/10.1021/bi301455k | *Biochemistry* 2013, 52, 1331−1343

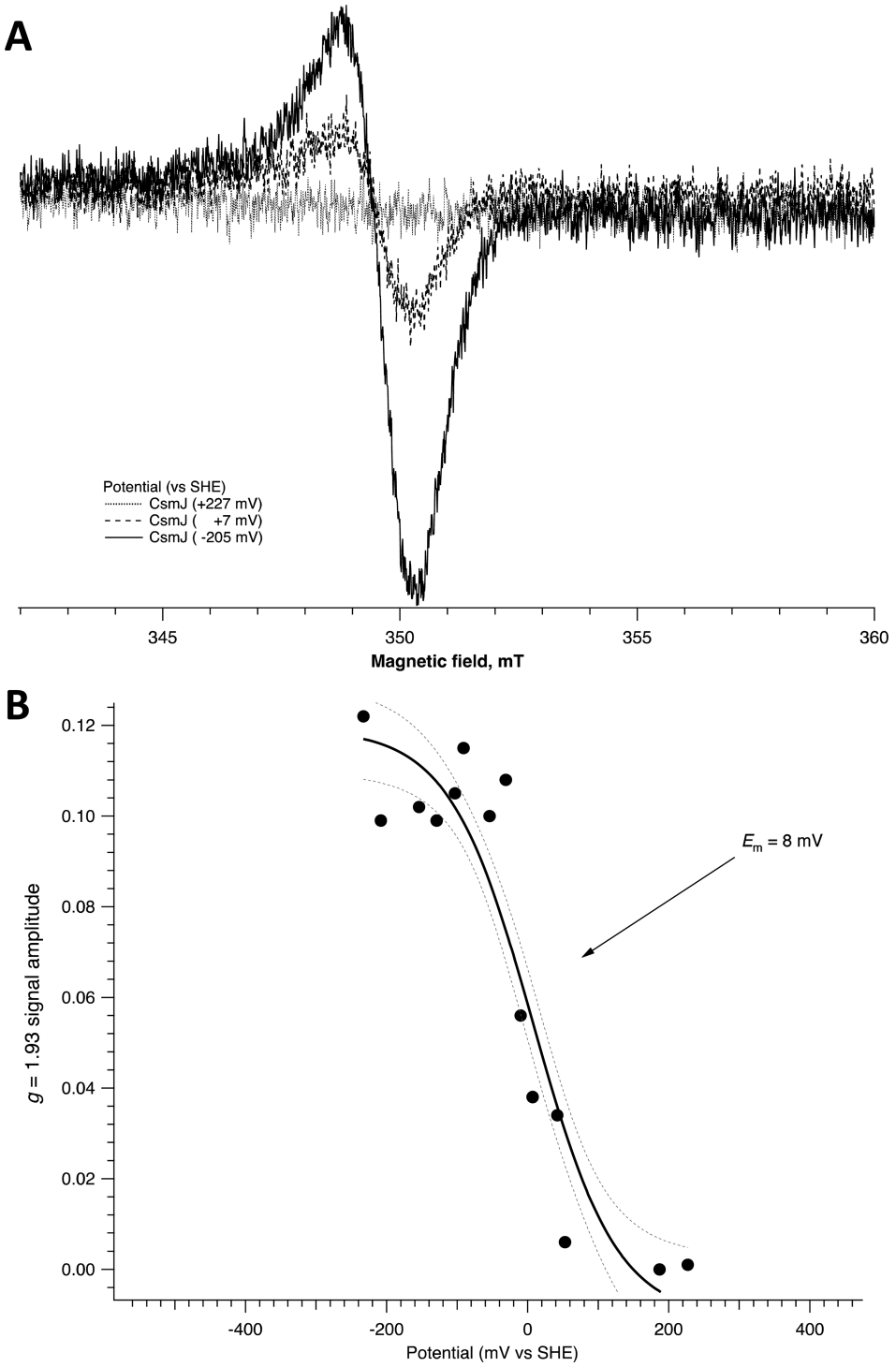

Figure 5. Representative EPR spectra of the CsmJ-containing chlorosomes at different solution potentials (A) and redox titration of isolated chlorosomes from the *csmI csmX* mutant (containing CsmJ) (B). For panel A, the potentials were adjusted stepwise by the addition of 50 mM sodium hydrosulfite. For panel B, the amplitude of the $g = 1.93$ EPR signal has been plotted against the potential of the solution as measured against the standard hydrogen electrode. Filled circles depict data from one experimental run at a given potential. The calculated curve fits are indicated by a solid line for the reduction potential and one-standard deviation error bars by flanking dashed lines. The curve is fit to a total of 14 points from two individual runs.

spectra for chlorosomes isolated from the *csmI csmJ csmX* triple mutant, which lacks all three Fe−S proteins, and chlorosomes from the *csmI csmJ* mutant that contain only CsmX is also shown in Figure 1B. The difference spectrum reveals a low-field g = 2.011 feature, which was assigned to the low-field peak of the Fe−S cluster in CsmX. Numerical simulation showed that CsmX has principal g values of 2.011, 1.933, and 1.929 (g_{av} = 1.958) with line widths of 1.0, 1.6, and 1.3 mT.

An organic radical, which appears in the EPR spectrum at g = 2.0036 with a 1.1 mT line width, is present in chemically reduced chlorosome samples. The intensity of this signal is sensitive to the redox potential of the solution. On the basis of its g value, the temperature independence of the signal, and its power saturation

dx.doi.org/10.1021/bi301455k | *Biochemistry* 2013, 52, 1331−1343

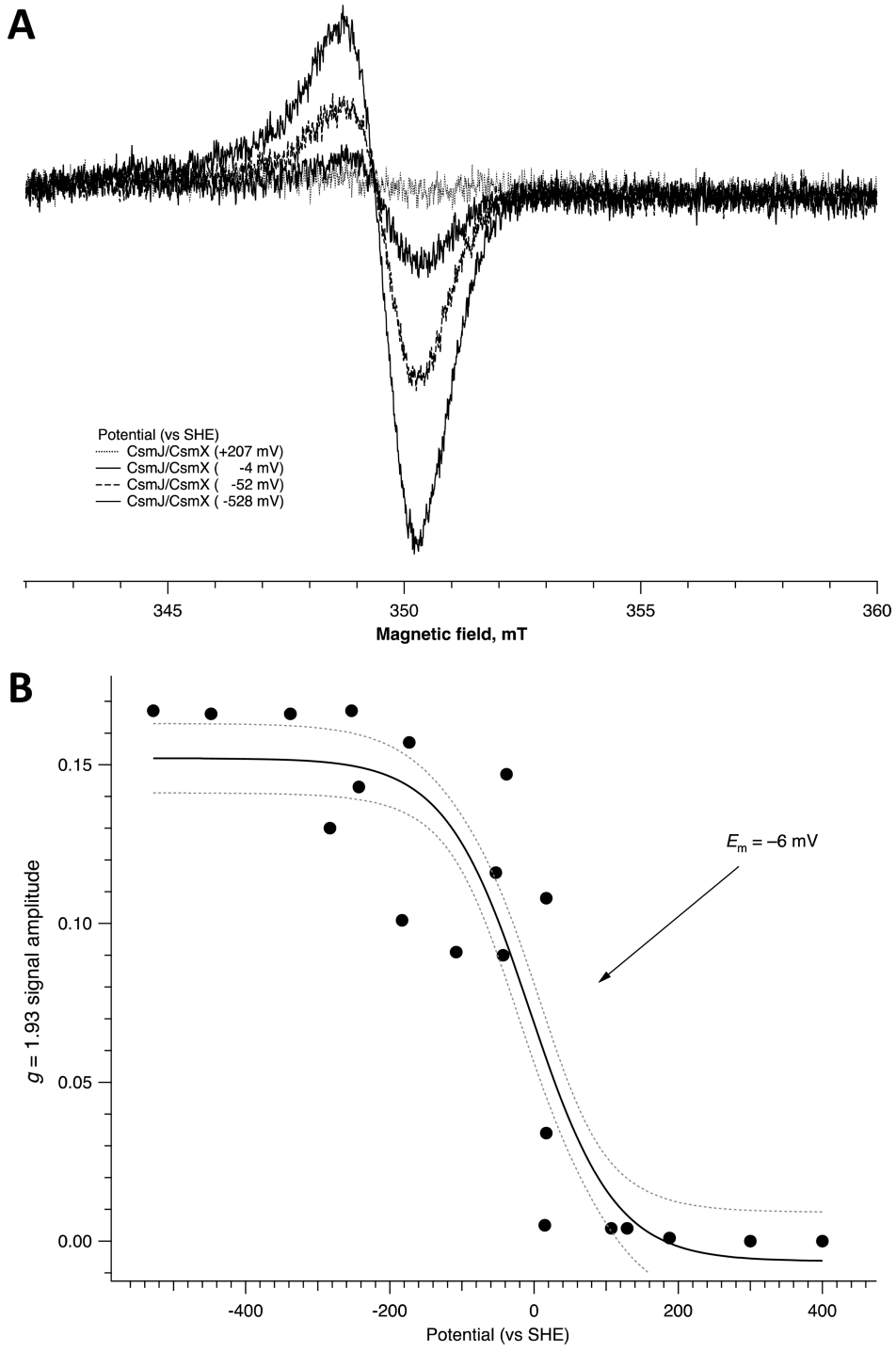

Figure 6. Representative EPR spectra of the CsmJ- and CsmX-containing chlorosomes at different solution potentials (A) and redox titration of isolated chlorosomes from the *csmI* mutant (containing CsmJ and CsmX) (B). For panel B, the potentials were adjusted stepwise by addition of 50 mM sodium hydrosulfite. For panel A, the amplitude of the $g = 1.93$ EPR signal has been plotted against the potential of the solution as measured against the standard hydrogen electrode. Filled circles depict data from one experimental run at a given potential. The calculated curve fits are indicated by a solid line for the reduction potential and one-standard deviation error bars by flanking dashed lines. The curve is fit to a total of 20 points from three individual runs.

behavior (data not shown), we concluded that this signal did not arise from any of the Fe–S clusters. The origin of this feature is uncertain, although it has a line width and a *g* value that are consistent with a semiquinone radical.

The EPR spectrum of chlorosomes from WT *Cba. tepidum* is a composite of the [2Fe-2S] clusters contained in the CsmI, CsmJ, and CsmX proteins, which can be simulated by summing the spectra of the individual chlorosomes on the basis of equal amounts of BChl *c*. On the basis of silver staining of SDS–PAGE gels, EPR signal amplitudes [see the preceding paper (DOI: 10.1021/bi301454g) and Figure 1A, and as reported in previous studies (e.g., refs 10 and 19)], approximately equal amounts of CsmI and CsmJ are present in the chlorosome envelope. Furthermore, cross-linking studies have shown that these two proteins form dimers, heterodimers, and $(CsmI)_2(CsmJ)_2$ heterotetramers.[10] Figure 2 shows the results of summing the

dx.doi.org/10.1021/bi301455k | *Biochemistry* 2013, 52, 1331–1343

individual, normalized EPR spectra for chlorosomes containing only CsmI or CsmJ. Figure 2A shows the sum of the experimental spectra, which accurately reproduces the features of the EPR spectrum of WT chlorosomes. The appropriately scaled spectrum of chlorosomes containing only CsmX has been included in the figure for comparison. Figure 2B shows the simulated spectrum of WT chlorosomes as a composite of the simulated CsmI and CsmJ spectra. In both panels of Figure 2, the WT spectrum is accurately represented as the sum of the spectra for chlorosomes containing CsmI and CsmJ in a 1:1 ratio. The simulations confirm that CsmX does not contribute any significant signal or feature to the EPR spectrum of WT chlorosomes.

Midpoint Potentials of WT Chlorosomes and Chlorosomes Lacking Specific Fe−S Cluster Proteins. The EPR spectrum of WT chlorosomes has a fairly broad feature between 347 and 349 mT when the clusters are fully reduced. Figure 3A shows that a pronounced change in the appearance of this feature occurs as the solution potential becomes more oxidizing. WT chlorosomes were fully reduced at −528 mV, and upon partial oxidation, this feature sharpened to yield a spectrum that closely resembled the spectrum of chlorosomes containing only CsmJ (see Figure 1A). On the basis of the simulation of the spectrum of WT chlorosomes, as well as the spectra of chlorosomes containing only CsmI or CsmJ, the signal that is lost upon partial oxidation clearly arises from CsmI. The remaining spectrum of the partially reduced WT chlorosomes matches that of CsmJ. Figure 3B depicts the amplitude of the high-field trough at 350.4 mT as a function of solution potential. Even though there is considerable scatter in the data, the fitted curve is consistent with the presence of two redox centers, one with a midpoint potential (E_{m1}) of −348 mV (n = 1) and the other with a midpoint potential (E_{m2}) of 92 mV (n = 1). The observed changes in the EPR spectra allow a direct assignment of the spectral features of the Fe−S clusters to specific proteins. The Fe−S cluster with the lower E_{m1} potential can be assigned to CsmI, and the Fe−S cluster with higher E_{m2} potential can be assigned to CsmJ. Correspondingly, these potentials are renamed E_{mI} and E_{mJ}, respectively. The EPR signal amplitudes for chlorosomes containing either CsmI or CsmJ were nearly equal, which is in good agreement with results from immunoblotting (DOI: 10.1021/bi301454g). Signals arising from the Fe−S cluster associated with CsmX were not observed during the redox titration experiments with WT chlorosomes.

Chlorosomes prepared from the three double mutants, *csmJ csmX*, *csmI csmX*, and *csmI csmJ*, have only one Fe−S protein in their envelopes, CsmI, CsmJ, and CsmX, respectively [see the preceding paper (DOI: 10.1021/bi301454g)]. Figure 4A shows the loss of the high-field feature of CsmI as the solution potential becomes more oxidizing. The spectral appearance confirms that these signals arise from the Fe−S cluster in CsmI. Figure 4B shows the amplitude of the high-field trough at 350.5 mT as a function of solution potential. The fitted data show that the [2Fe-2S] cluster in CsmI titrates with a midpoint potential of −205 mV (n = 1). Figure 5A shows the loss of the high-field feature of CsmJ as the solution potential becomes more oxidizing. The spectral appearance confirms these signals arise from the Fe−S cluster in CsmJ. Figure 5B shows the amplitude of the high-field trough at 350.3 mT as a function of solution potential. The fitted data show that the [2Fe-2S] cluster in CsmJ titrates with a midpoint potential of 8 mV (n = 1). The midpoint potential of the [2Fe-2S] cluster in CsmX in chlorosomes isolated from the *csmI csmJ* double mutant was estimated to be more oxidizing than −180 mV (data not shown). Because of the very low concentration of CsmX in chlorosomes, it was not possible to determine accurately the midpoint potential of the Fe−S cluster in this protein.

The midpoint potentials determined for the Fe−S clusters in the individual CsmI and CsmJ proteins do not match the midpoint potentials observed in WT chlorosomes. However, consistent with the observations for WT chlorosomes, the [2Fe-2S] cluster in CsmI had a lower redox potential (−205 mV) and the [2Fe-2S] cluster in CsmJ had a higher redox potential (8 mV). The possible reasons for these differences will be described in the Discussion.

Given the differences in the midpoint potentials of the Fe−S clusters in WT chlorosomes and chlorosomes containing either CsmI or CsmJ alone, a check was conducted by performing redox titrations on chlorosomes isolated from the *csmI* mutant, which contains both CsmJ and CsmX [see preceding paper (DOI: 10.1021/bi301454g)]. Figure 6A shows the loss of the high-field feature of CsmJ as the solution potential becomes more oxidizing. The spectral appearance confirms that this signal arises primarily from the Fe−S cluster in CsmJ. Figure 6B shows the amplitude of the high-field trough at 350.3 mT as a function of solution potential. The fitted data show that the predominant [2Fe-2S] cluster in these chlorosomes has a midpoint potential of −6 mV (n = 1), a value only 14 mV from that for CsmJ in the *csmI csmX* mutant (8 mV). Furthermore, the amplitude of the signals observed in the g = 1.93 region are comparable to those in the chlorosomes of the *csmI csmX* double mutant, which contain only CsmJ. Neither the midpoint potential nor the EPR spectrum revealed any contribution from CsmX.

DISCUSSION

Ferredoxins containing [2Fe-2S] clusters are typically small, soluble proteins that participate in diverse metabolic reactions in virtually all organisms. They are classified by structure and function into plant-type,[32] vertebrate-type,[33,34] and thioredoxin-type ferredoxins.[35,36] Plant-type ferredoxins are found in chloroplasts and cyanobacteria, and these proteins transfer electrons from photosystem I to ferredoxin:NADP$^+$ reductase during photosynthesis.[37] They also serve as electron donors to various cellular enzymes involved in nitrogen, sulfur, and amino acid metabolism.[38−40] Vertebrate-type ferredoxins include the ferredoxins in mammalian mitochondria (e.g., adrenodoxin) and some bacterial ferredoxins (e.g., putidaredoxin). They carry electrons from ferredoxin reductases to membrane-bound cytochrome P450 in mitochondria or to various soluble cytochromes P450 in bacteria that catalyze hydroxylation reactions.[41] Although the level of sequence similarity between plant-type and vertebrate-type [2Fe-2S] ferredoxins is low (<23%), these proteins nevertheless share the same structural framework.[34,41] In both cases, the N-terminal and C-terminal halves of the polypeptides form two "lobes", and the binding site for the Fe−S cluster is located between the lobes at one end of the molecule.[42] Thioredoxin-type ferredoxins were first discovered in late 1980s and were defined structurally by the X-ray structure of a representative from *Aquifex aeolicus*.[35,36] Many uncertainties remain regarding the function(s) of thioredoxin-type ferredoxins, and it is unclear whether they participate in redox regulation or electron transfer reactions.[36]

The chlorosome proteins CsmI and CsmJ contain [2Fe-2S] clusters and possess a conserved motif that is typical of vertebrate-type [2Fe-2S] ferredoxins, CggxxxCxtCx-X$_{33-36}$-C, in their N-terminal domains.[18] CsmX also exhibits sequence

similarity to vertebrate-type ferredoxins, although it has been less well characterized because of its low abundance in chlorosomes [see preceding paper (DOI: 10.1021/bi301454g)]. Vassilieva et al.[14,18] suggested that these three Fe−S proteins comprised an adrenodoxin domain and a CsmA/E-like domain that served to anchor the proteins in the chlorosome envelope. Cross-linking studies provided strong evidence of the formation of CsmI and CsmJ homodimers, heterodimers, and heterotetramers [$(CsmI)_2(CsmJ)_2$].[10] Although *csmI*, *csmJ*, and *csmX* single mutants had previously been partly characterized,[19] further progress in performing genetic manipulations in *Cba. tepidum* allowed us to extend these initial studies and to characterize the [2Fe-2S] clusters of CsmI, CsmJ, and CsmX of the chlorosome envelope more thoroughly. Several new mutant strains, which lacked some or all of the proteins harboring Fe−S clusters, were constructed and characterized [see the preceding paper (DOI: 10.1021/bi301454g) and Table 1]. The new mutant strains produced chlorosomes containing two, one, or no proteins containing Fe−S clusters. In principle, these mutants should allow characterization of each Fe−S protein in its native state in the chlorosome envelope.

Table 1. Midpoint Potentials of the [2Fe-2S] Clusters in Chlorosome Proteins of *Cba. tepidum*

strain	chlorosome protein	midpoint potential
wild type	CsmI, CsmJ, CsmX	E_{mI} = −348 mV E_{mJ} = 92 mV
csmJ csmX	CsmI	E_m = −205 mV
csmI csmX	CsmJ	E_m = 8 mV
csmI csmJ	CsmX	E_m > −180 mV
csmI	CsmJ, CsmX	E_m = −6 mV
csmI csmJ csmX	none	none

Under reducing conditions, purified chlorosomes containing either CsmI or CsmJ exhibited distinctive EPR spectra. These spectra were sufficiently detailed to resolve and compare the principal *g* values associated with each protein, 2.017, 1.942, and 1.929 for CsmI and 2.019, 1.935, and 1.933 for CsmJ (Figure 1A). These values were used to assign a specific cluster to the midpoint potentials for chlorosomes containing CsmI and/or CsmJ. Because CsmX occurs in much smaller amounts (~5% in the chlorosome envelopes of *Cba. tepidum* compared to the amount of CsmI and CsmJ combined), EPR signals arising from the derivative and high-field trough of CsmX were very difficult to observe and were visible only when BChl *c* concentrations exceeded 30 mg of BChl *c*/mL. After the broad derivative spectrum of an organic radical at $g = 2.0036$ had been subtracted, a feature assigned to the low-field peak ($g = 2.011$) of CsmX could be observed (see Figure 1B).

The EPR spectrum of the Fe−S clusters in WT chlorosomes could be accurately simulated in this study by simply summing the spectra of chlorosomes containing the individual Fe−S proteins. Combining the spectra for CsmI and CsmJ in a 1:1 ratio accurately reproduced the spectrum of WT chlorosomes (Figure 2B). CsmX was not included in these simulations because it had a negligible contribution to the EPR spectrum in WT chlorosomes. The contribution of the individual Fe−S clusters can readily be observed in the admixture of the CsmI and CsmJ spectra, and differences in the simulations could probably be discerned for differences of <5% in the ratio of these two proteins. This level of resolution allowed a measurement of the oxidation−reduction states of the two Fe−S clusters.

A previous comparison of the EPR spectral properties of CsmI and CsmJ in inclusion bodies after heterologous expression in *E. coli* and of the native proteins in chlorosomes showed relatively minor differences.[18] On the basis of numerical simulations, the principal *g* values and line widths of the Fe−S cluster in CsmJ differed only slightly for these two cases. Numerical simulation of CsmI in inclusion bodies was not possible because of its low solubility and because of the low occupancy of Fe−S clusters in this protein. Nevertheless, a visual comparison of the two spectra for CsmI revealed comparable principal *g* values and line widths. The minor differences in the EPR spectra were attributed to the distinctly different protein environments.[18]

It was previously reported that the midpoint potentials for the Fe−S clusters in WT chlorosomes were as follows: E_{m1} = −201 mV, and E_{m2} = 92 mV.[18] The results for redox titration of Fe−S clusters in WT chlorosomes in this study differ in two ways from those of the previous study.[18] In both studies, one of the observed midpoint potentials (E_{m2}) was ~90 mV. Vassilieva et al.[18] assigned E_{m1} to CsmJ, because the midpoint potential of recombinant CsmJ in inclusion bodies (−194 mV) was similar to the lower of the two midpoint potentials observed in WT chlorosomes (−201 mV). On the basis of differences in the EPR spectra (Figure 2), this study assigns E_{m2} (92 mV) to CsmJ and E_{m1} (−348 mV) to CsmI. The second major difference between the two studies is the much greater reducing midpoint potential for E_{m1} (−348 mV vs −201 mV). The 147 mV difference in these midpoint potentials may have partly arisen because too much importance was assigned to the midpoint potential values for recombinant CsmJ in inclusion bodies. The data plotted in the redox titration presented in Figure 7B of Vassilieva et al.[18] were derived from two independent sets of titration data. The first data set was in excellent agreement with the potentials inferred for WT chlorosomes in this study. Two midpoint potentials were observed, and the calculated midpoint potentials were as follows: E_{m1} = −356 mV, and E_{m2} = 72 mV. Because these data did not agree with the results shown for CsmJ in Figure 7A of ref 18, additional titration experiments were performed, and the additional data points were combined with the original data. It is now clear from a close re-examination of these data, however, that the second data set was much noisier and scattered than the first, especially in the range from −500 to −50 mV. The inclusion of these additional data fortuitously raised the average midpoint potential for E_{m1} to −201 mV, which coincidentally was a good match to the midpoint potential of CsmJ in inclusion bodies.

In this study, the midpoint potentials of the Fe−S clusters in WT chlorosomes differed markedly from the values for the same proteins in chlorosomes of mutants containing only one Fe−S protein. For example, the midpoint potential of CsmI in chlorosomes isolated from the *csmJ csmX* mutant was more than 140 mV more positive than the midpoint potential of CsmI (E_{mI}) in WT chlorosomes. Conversely, the midpoint potential of CsmJ in chlorosomes isolated from the *csmI csmX* mutant was more than 80 mV more negative than the midpoint potential of CsmJ (E_{mJ}) in WT chlorosomes (Table 1).

There are several possible explanations for the observed midpoint potential differences of these Fe−S cluster-containing proteins. Recombinant CsmJ in inclusion bodies had a midpoint potential E_m of −194 mV,[18] and CsmJ embedded in the envelopes of WT chlorosomes had a midpoint potential E_m of 90 mV. Two mutants (*csmI csmX* and *csmX*) producing chlorosomes containing CsmJ showed comparable midpoint potentials (E_m values of −6 and 8 mV, respectively). CsmJ, therefore, has been shown to have three distinct redox potentials that span nearly

300 mV. If one assumes that the protein is essentially unchanged, then the wide variation of midpoint potentials must be attributed to changes in the local environment surrounding the Fe−S cluster. The solvent accessibility of Fe−S clusters is believed to modulate the midpoint potentials of ferredoxins; increasingly negative redox potentials are believed to result from the decreased solvent accessibility of the Fe−S clusters.[43] CsmJ was up to ∼200 mV more reducing when it occurred in insoluble inclusion bodies than when it occurred as the only Fe−S protein in chlorosome envelopes.[18] These observations suggest that the Fe−S cluster in CsmJ in WT chlorosomes may be more exposed than when it occurs alone in chlorosome envelopes or in inclusion bodies.

On the basis of SDS−PAGE and immunoblotting analyses [see preceding paper (DOI: 10.1021/bi301454g)], the relative amounts of chlorosome envelope proteins other than the Fe−S proteins were unaffected by the double and triple mutations introduced in this study. This suggests that any redox potential shift must arise from interactions that occur between or among the three Fe−S proteins. Previous cross-linking studies showed that CsmI and CsmJ can form dimers, and strong evidence of the occurrence of CsmI−CsmJ heterodimers and $(CsmI)_2(CsmJ)_2$ heterotetramers was also obtained from cross-linking.[10] Thus, it is reasonable to propose that the different midpoint potentials observed arise from the formation of homodimers, heterodimers, and heterotetramers of these two Fe−S cluster-containing proteins. Given three Fe−S proteins, a total of six possible combinations of homodimers and heterodimers are possible. However, most of these combinations can be excluded because of the much lower levels of CsmX than of CsmI and CsmJ. For example, chlorosomes of the *csmI* mutant contain both CsmJ and CsmX [see preceding paper (DOI: 10.1021/bi301454g)], but the observed potential of −6 mV was similar to the value of 8 mV observed in chlorosomes of the *csmI csmX* double mutant that contained only CsmJ. Thus, CsmX has no significant effect on the midpoint potential of the Fe−S clusters in CsmJ. On the basis of the studies presented here, the Fe−S clusters in CsmI homodimers have a midpoint potential of approximately −200 mV and the Fe−S clusters in CsmJ homodimers have a midpoint potential of approximately 8 mV (Table 1).

Energy transfer in chlorosomes is strongly quenched under oxic conditions, which presumably functions as a defense mechanism against oxidative damage as cells are exposed to O_2.[23−26] Studies of the kinetics of energy transfer quenching (detected as quenching of fluorescence emission) and the recovery of energy transfer (detected as recovery of fluorescence emission) strongly implicate two Fe−S proteins, CsmI and CsmJ, as playing roles in the electron transfer processes that control energy transfer when cells (or chlorosomes) have been exposed to oxygen [see preceding paper (DOI: 10.1021/bi301454g)]. Isoprenoid quinones closely associated with BChl *c* in chlorosomes have been proposed as the redox-sensitive quencing species.[21,26] If oxidized quinones are the quenchers of energy transfer, reduction of oxidized menaquinone or chlorobiumquinones would be necessary to reactivate energy transfer after cells or chlorosomes have been exposed to oxygen. In *Cba. tepidum*, complexes of CsmI and CsmJ might be responsible for the reduction of these quinones after exposure to oxygen, presumably using electrons derived from the abundant, soluble 2[4Fe-4S] ferredoxins in the cytoplasm of *Cba. tepidum*.[5] The midpoint potential for quenching fluorescence in chlorosomes of *Cba. tepidum* is approximately −100 mV[25] and is similar in chlorosomes of other green sulfur bacteria.[24] On the basis of the midpoint potentials discussed here and depending upon the conditions, the Fe−S clusters in a heterotetramer of CsmI and CsmJ could function in either oxidation or reduction of the quencher present in chlorosomes. This suggestion is supported by the observations made in the preceding study (DOI: 10.1021/bi301454g).

No specific function was identified for CsmX in chlorosomes of *Cba. tepidum*, and elimination of this protein by insertional inactivation of its gene had an only minor effect on the energy transfer properties of chlorosomes that still contained CsmI and CsmJ [see preceding paper (DOI: 10.1021/bi301454g)]. However, when the genomes of 17 chlorosome-producing members of the phylum Chlorobi were surveyed, it was found that 13 of them encode orthologs of *csmI*, *csmJ*, and *csmX*. *Chlorobium chlorochromatii*, the epibiont of the phototrophic consortium "*Chlorochromatium aggregatum*",[44] does not have a *csmJ* gene, which was possibly deleted during a recombination event. *Chlorobium phaeovibrioides* DSM 265 has retained the dicistronic *csmJX* operon but does not have the *csmI* gene. The *Chloroherpeton thalassium* genome encodes two similar Fe−S proteins in a dicistronic operon, but these proteins are rather distantly related to the *csmI*, *csmJ*, and *csmX* proteins described here. Finally, "*Candidatus* Thermochlorobacter aerophilum" is missing *csmJ* but apparently has distant homologues of *csmI* and *csmX*.[45] Thus, no specific pattern that associated Fe−S protein content with specific functionalities was evident from the gene distribution analysis, but the results certainly imply that CsmX has a specific function and might substitute for CsmI or CsmJ in some cases. Further studies of isolated complexes will be required to determine which complexes are involved in the oxidation and reduction of quinones in chlorosomes in green sulfur bacteria.

The genome of "*Candidatus* Chloracidobacterium thermophilum" encodes a single adrenodoxin-like, Fe−S protein (Cabther_A2114), which is localized in chlorosome envelopes.[46] Interestingly, the chlorosome envelopes of this acidobacterium additionally contain a type II NADH dehydrogenase (Cabther_B0793), which could transfer electrons from NADH to (or from) the putative quinone quencher, menaquinone-7.[46,47] These two proteins could either provide alternative pathways for oxidation and reduction of the quencher or specific pathways for oxidation or reduction of the quencher. A single gene, Caur_0356, also encodes an Fe−S protein putatively associated with the chlorosome envelopes of *Chloroflexus aurantiacus* strain j-10-fl. Orthologs of Caur_0356 are found in other chlorosome-producing members of the Chloroflexi (*Chloroflexus aggregans*, *Chloroflexus aurantiacus* Y-400, and *Oscillochloris trichoides*). However, *Roseiflexus* spp., which do not produce chlorosomes,[5] do not have a similar gene. The *Cfx. aurantiacus* genome also encodes a type II NADH dehydrogenase (Caur_0141), which could transfer electrons from NADH to and/or from chlorosome-localized menaquinone-10 in this facultatively anoxygenic phototroph.[26,46] This gene is clustered with genes encoding several proteins of the chlorosome envelope, including CsmM (Caur_0139), CsmN (Caur_0140), and CsmP (Caur_0142).[5] Metabolic processes occurring in "*Candidatus* Chloracidobacterium thermophilum" and *Cfx. aurantiaus* are much less dependent on highly reducing ferredoxins,[5] and this could be a reason for these organisms to utilize type II NADH dehydrogenases to oxidize and reduce the quinone quenchers in their chlorosomes. Although *Cba. tepidum* encodes a type II NADH dehydrogenase (CT0369), there is currently no evidence that this enzyme exists in chlorosomes.

In conclusion, the envelopes of chlorosomes contain Fe−S proteins that play important roles in the oxidation and reduction of the quencher that occur in chlorosomes. Upon exposure of cells to oxygen, oxidized quinones rapidly quench energy transfer, which minimizes the formation of reactive oxygen species in the cells. To reactivate energy transfer, mechanisms must exist to reduce the quenching species. CsmI and CsmJ are components of a light-dependent mechanism that connects intracellular reductants to the reduction of the oxidized (active) quencher [see preceding paper (DOI: 10.1021/bi301454g)]. As shown here, the redox properties of these Fe−S proteins are well suited for this task.

AUTHOR INFORMATION

Corresponding Author

*Department of Biochemistry and Molecular Biology, 108 Althouse Laboratory, The Pennsylvania State University, University Park, PA 16802. Phone: (814) 865-1992. Fax: (814) 863-7024. E-mail: dab14@psu.edu.

Present Addresses

[‖]Department of Chemistry, Susquehanna University, Selinsgrove, PA 17870.

[⊥]Section for Marine Biology, Department of Genome Sciences, University of Washington, Seattle, WA 98195.

[@]Department of Biology, University of Copenhagen, Strandpromenaden 5, 3000 Helsingør, Denmark.

Funding

This work was supported by grants from the U.S. Department of Energy (DE-FG02-94ER20137 to D.A.B. and DE-FG02-08ER15989 to J.H.G.).

Notes

The authors declare no competing financial interests.

ABBREVIATIONS

BChl, bacteriochlorophyll; DMSO, dimethyl sulfoxide; EPR, electron paramagnetic resonance; FMO, Fenna−Matthews−Olson protein; PAGE, polyacrylamide gel electrophoresis; SDS, sodium dodecyl sulfate; WT, wild type or wild-type.

REFERENCES

(1) Blankenship, R. E., and Matsuura, K. (2003) Antenna complexes from green photosynthetic bacteria. In *Advances in Photosynthesis and Respiration, Vol. 13, Light-Harvesting Antennas* (Green, B. R., and Parson, W. W., Eds.) pp 195−217, Kluwer, Dordrecht, The Netherlands.

(2) Frigaard, N.-U., and Bryant, D. A. (2006) Chlorosomes: Antenna organelles in photosynthetic green bacteria. In *Microbiology Monographs, Vol. 2, Complex Intracellular Structures in Prokaryotes* (Shively, J. M., Ed.) pp 79−114, Springer, Berlin.

(3) Bryant, D. A., Garcia Costas, A. M., Maresca, J. A., Chew, A. G., Klatt, C. G., Bateson, M. M., Tallon, L. J., Hostetler, J., Nelson, W. C., Heidelberg, J. F., and Ward, D. M. (2007) *Candidatus* Chloracidobacterium thermophilum: An aerobic phototrophic Acidobacterium. *Science 317*, 523−526.

(4) Oostergetel, G. T., van Amerongen, H., and Boekema, E. J. (2010) The chlorosome: A prototype for efficient light harvesting in photosynthesis. *Photosynth. Res. 104*, 245−255.

(5) Bryant, D. A., Liu, Z., Li, T., Zhao, F., Garcia Costas, A. M., Klatt, C. G., Ward, D. M., Frigaard, N.-U., and Overmann, J. (2012). Comparative and functional genomics of anoxygenic green bacteria from the taxa *Chlorobi*, *Chloroflexi*, and *Acidobacteria*. In *Advances in Photosynthesis and Respiration, Vol. 35, Functional Genomics and Evolution of Photosynthetic Systems* (Burnap, R. L., and Vermaas, W., Eds.) pp 47−102, Springer, Dordrecht, The Netherlands.

(6) Martinez-Planells, A., Arellano, J. B., Borrego, C. M., López-Iglesias, C., Gich, F., and Garcia-Gil, J. (2002) Determination of the topography and biometry of chlorosomes by atomic force microscopy. *Photosynth. Res. 71*, 83−90.

(7) Montaño, G. A., Bowen, B. P., LaBelle, J. T., Woodbury, N. W., Pizziconi, V. B., and Blankenship, R. E. (2003) Characterization of *Chlorobium tepidum* chlorosomes: A calculation of bacteriochlorophyll *c* per chlorosome and oligomer modeling. *Biophys. J. 8*, 2560−2565.

(8) Ganapathy, S., Oostergetel, G. T., Wawrzyniak, P. K., Reus, M., Gomez Maqueo Chew, A., Buda, F., Boekema, E. J., Bryant, D. A., Holzwarth, A. R., and de Groot, H. J. M. (2009) Alternating *syn-anti* bacteriochlorophylls form concentric helical nanotubes in chlorosomes. *Proc. Natl. Acad. Sci. U.S.A. 106*, 8525−8530.

(9) Ganapathy, S., Reus, M., Oostergetel, G., Wawrzyniak, P. K., Tsukatani, Y., Gomez Maqueo Chew, A., Buda, F., Bryant, D. A., Holzwarth, A. R., and de Groot, H. J. M. (2012) Structural Variability in Wild-Type and *bchQ bchR* Mutant Chlorosomes of the Green Sulfur Bacterium Chlorobaculum tepidum. *Biochemistry 51*, 4488−4498.

(10) Li, H., Frigaard, N.-U., and Bryant, D. A. (2006) Molecular contacts for chlorosome envelope proteins revealed by cross-linking studies with chlorosomes from *Chlorobium tepidum*. *Biochemistry 45*, 9095−9103.

(11) Pedersen, M. Ø., Linnanto, J., Frigaard, N.-U., Nielsen, N. C., and Miller, M. (2010) A model of the protein-pigment baseplate complex in chlorosomes of photosynthetic green bacteria. *Photosynth. Res. 104*, 233−243.

(12) Wen, J., Zhang, H., Gross, M. L., and Blankenship, R. E. (2009) Membrane orientation of the FMO antenna protein from *Chlorobaculum tepidum* as determined by mass spectrometry-based footprinting. *Proc. Natl. Acad. Sci. U.S.A. 106*, 6134−6139.

(13) Bryant, D. A., Vassilieva, E. V., Frigaard, N.-U., and Li, H. (2002) Selective protein extraction from *Chlorobium tepidum* chlorosomes using detergents. Evidence that CsmA forms multimers and binds bacteriochlorophyll *a*. *Biochemistry 41*, 14403−14411.

(14) Vassilieva, E. V., Stirewalt, V. L., Jakobs, C. U., Frigaard, N.-U., Inoue-Sakamoto, K., Baker, M. A., Sotak, A., and Bryant, D. A. (2002) Subcellular localization of chlorosome proteins in *Chlorobium tepidum* and characterization of three new chlorosome proteins: CsmF, CsmH, CsmX. *Biochemistry 41*, 4358−4370.

(15) Chung, S., Frank, G., Zuber, H., and Bryant, D. A. (1994) Genes encoding two chlorosome components from the green sulfur bacteria *Chlorobium vibrioforme* strain 8327d and *Chlorobium tepidum*. *Photosynth. Res. 41*, 261−275.

(16) Chung, S., and Bryant, D. A. (1996) Characterization of *csmB* genes, encoding a 7.5-kDa protein of the chlorosome envelope, from the green sulfur bacteria *Chlorobium vibrioforme* 8327d and *Chlorobium tepidum*. *Arch. Microbiol. 166*, 234−244.

(17) Chung, S., and Bryant, D. A. (1996) Characterization of the *csmD* and *csmE* genes from *Chlorobium tepidum*. The CsmA, CsmC, CsmD, and CsmE proteins are components of the chlorosome envelope. *Photosynth. Res. 50*, 41−59.

(18) Vassilieva, E. V., Antonkine, M. L., Zybailov, B. L., Yang, F., Jakobs, C. U., Golbeck, J. H., and Bryant, D. A. (2001) Electron transfer may occur in the chlorosome envelope: The CsmI and CsmJ proteins of chlorosomes are 2Fe-2S ferredoxins. *Biochemistry 40*, 464−473.

(19) Frigaard, N.-U., Li, H., Milks, K. J., and Bryant, D. A. (2004) Nine mutants of *Chlorobium tepidum* each unable to synthesize a different chlorosome protein still assemble functional chlorosomes. *J. Bacteriol. 186*, 646−653.

(20) Li, H., and Bryant, D. A. (2009) Envelope proteins of the CsmB/CsmF and CsmC/CsmD motif families influence the size, shape, and composition of chlorosomes in *Chlorobaculum tepidum*. *J. Bacteriol. 191*, 7109−7120.

(21) Frigaard, N.-U., Takaichi, S., Hirota, M., Shimada, K., and Matsuura, K. (1997) Quinones in chlorosomes of green sulfur bacteria and their role in the redox-dependent fluorescence studied in chlorosome like bacteriochlorophyll *c* aggregates. *Arch. Microbiol. 167*, 343−349.

(22) Frigaard, N.-U., Matsuura, K., Hirota, M., Miller, M., and Cox, R. P. (1998) Studies of the location and function of isoprenoid quinones in chlorosomes from green sulfur bacteria. *Photosynth. Res. 58*, 81−90.
(23) Wang, J., Brune, D. C., and Blankenship, R. E. (1990) Effects of oxidants and reductants on the efficiency of excitation transfer in green photosynthetic bacteria. *Biochim. Biophys. Acta 1015*, 457−463.
(24) Blankenship, R. E., Cheng, P., Causgrove, T. P., Brune, D. C., Wang, S. H. H., Choh, J.-U., and Wang, J. (1993) Redox regulation of energy transfer efficiency in antennas of green photosynthetic bacteria. *Photochem. Photobiol. 57*, 103−107.
(25) Frigaard, N.-U., and Matsuura, K. (1999) Oxygen uncouples light absorption by the chlorosome antenna and photosynthetic electron transfer in the green sulfur bacterium *Chlorobium tepidum*. *Biochim. Biophys. Acta 1412*, 108−117.
(26) Frigaard, N.-U., Tokita, S., and Matsuura, K. (1999) Exogenous quinones inhibit photosynthetic electron transfer in *Chloroflexus aurantiacus* by specific quenching of the excited bacteriochlorophyll *c* antenna. *Biochim. Biophys. Acta 1413*, 108−116.
(27) Wahlund, T. M., Woese, C. R., Castenholz, R. W., and Madigan, M. T. (1991) A thermophilic green sulfur bacterium from New Zealand hot springs, *Chlorobium tepidum* sp. nov. *Arch. Microbiol. 156*, 81−90.
(28) Wahlund, T. M., and Madigan, M. T. (1995) Genetic transfer by conjugation in the thermophilic green sulfur bacterium *Chlorobium tepidum*. *J. Bacteriol. 177*, 2583−2588.
(29) Frigaard, N.-U., and Bryant, D. A. (2001) Chromosomal gene inactivation in the green sulfur bacterium *Chlorobium tepidum* by natural transformation. *Appl. Environ. Microbiol. 67*, 2538−2544.
(30) Gerola, P. D., and Olson, J. M. (1986) A new bacteriochlorophyll *a*-protein complex associated with chlorosomes of green sulfur bacteria. *Biochim. Biophys. Acta 848*, 69−76.
(31) Stanier, R. Y., and Smith, J. H. C. (1960) The chlorophylls of green bacteria. *Biochim. Biophys. Acta 41*, 478−484.
(32) Morales, R., Charon, M.-H., Hudry-Clergeon, G., Petillot, Y., Norager, S., Medina, M., and Frey, M. (2000) Refined X-ray structures of the oxidized, at 1.3 Å, and reduced, at 1.17 Å, [2Fe-2S] ferredoxin from the cyanobacterium *Anabaena* PCC7119 show redox-linked conformational changes. *Biochemistry 39*, 2428−2428.
(33) Müller, A., Müller, J. J., Muller, Y. A., Uhlmann, H., Bernhardt, R., and Heinemann, U. (1998) New aspects of electron transfer revealed by the crystal structure of a truncated bovine adrenodoxin, Adx(4−108). *Structure 6*, 269−280.
(34) Grinberg, A. V., Hannemann, F., Schiffler, B., Muller, J., Heinemann, U., and Bernhardt, R. (2000) Adrenodoxin: Structure, stability, and electron transfer properties. *Proteins 40*, 590−612.
(35) Yeh, A. P., Chatelet, C., Soltis, S. M., Kuhn, P., Meyer, J., and Rees, D. C. (2000) Structure of a thioredoxin-like [2Fe-2S] ferredoxin from *Aquifex aeolicus*. *J. Mol. Biol. 300*, 587−595.
(36) Meyer, J. (2001) Ferredoxins of the third kind. *FEBS Lett. 509*, 1−5.
(37) Xu, W., Tang, H., Wang, Y., and Chitnis, P. R. (2001) Proteins of the cyanobacterial photosystem I. *Biochim. Biophys. Acta 1507*, 32−40.
(38) Nakayama, M., Akashi, T., and Hase, T. (2000) Plant sulfite reductase: Molecular structure, catalytic function and interaction with ferredoxin. *J. Inorg. Biochem. 82*, 27−32.
(39) Hirasawa, M., Rubio, L. M., Griffin, J. L., Flores, E., Herrero, A., Li, J., Kim, S. K., Hurley, J. K., Tollin, G., and Knaff, D. B. (2004) Complex formation between ferredoxin and *Synechococcus* ferredoxin: Nitrate oxidoreductase. *Biochim. Biophys. Acta 1608*, 155−162.
(40) van den Heuvel, R. H., Svergun, D. I., Petoukhov, M. V., Coda, A., Curti, B., Ravasio, S., Vanoni, M. A., and Mattevi, A. (2003) The active conformation of glutamate synthase and its binding to ferredoxin. *J. Mol. Biol. 330*, 113−128.
(41) Sevrioukova, I. F., Garcia, C., Li, H., Bhaskar, B., and Poulos, T. L. (2003) Crystal structure of putidaredoxin, the [2Fe-2S] component of the P450cam monooxygenase system from *Pseudomonas putida*. *J. Mol. Biol. 333*, 377−392.
(42) Kostic, M., Pochapsky, S. S., Obenauer, J., Mo, H., Pagani, G. M., Pejchal, R., and Pochapsky, T. C. (2002) Comparison of functional domains in vertebrate-type ferredoxins. *Biochemistry 41*, 5978−5989.
(43) Stephens, P. J., Jollie, D. R., and Warshel, A. (1996) Protein control of redox potentials of iron-sulfur proteins. *Chem. Rev. 96*, 2491−2514.
(44) Vogl, K., Glaeser, J., Pfannes, K. R., Wanner, G., and Overmann, J. (2006) *Chlorobium chlorochromatii* sp. nov., a symbiotic green sulfur bacterium isolated from the phototrophic consortium "*Chlorochromatium aggregatum*". *Arch. Microbiol. 185*, 363−372.
(45) Liu, Z., Klatt, C. G., Ludwig, M., Rusch, D. B., Jensen, S. I., Kühl, M., Ward, D. M., and Bryant, D. A. (2012) "*Candidatus* Thermochlorobacter aerophilum": An aerobic chlorophotoheterotrophic member of the phylum Chlorobi defined by metagenomics and metatranscriptomics. *ISME J. 6*, 1869−1882.
(46) Garcia Costas, A. M., Tsukatani, Y., Romberger, S. P., Oostergetel, G., Boekema, E., Golbeck, J. H., and Bryant, D. A. (2011) Ultrastructural analysis and identification of envelope proteins of "*Candidatus* Chloracidobacterium thermophilum" chlorosomes. *J. Bacteriol. 193*, 6701−6711.
(47) Garcia Costas, A. M., Tsukatani, Y., Rijpstra, W. I. C., Schouten, S., Welander, P. V., Summons, R. E., and Bryant, D. A. (2012) Identification of the bacteriochlorophylls, carotenoids, quinones, lipids, and hopanoids of "*Candidatus* Chloracidobacterium thermophilum". *J. Bacteriol. 194*, 1158−1168.